Photochemistry |Hot Paper|

Controlling Spin-Correlated Radical Pairs with Donor–Acceptor Dyads: A New Concept to Generate Reduced Metal Complexes for More Efficient Photocatalysis

Svenja Neumann,[a] Oliver S. Wenger,*[a] and Christoph Kerzig*[a, b]

Abstract: One-electron reduced metal complexes derived from photoactive ruthenium or iridium complexes are important intermediates for substrate activation steps in photoredox catalysis and for the photocatalytic generation of solar fuels. However, owing to the heavy atom effect, direct photochemical pathways to these key intermediates suffer from intrinsic efficiency problems resulting from rapid geminate recombination of radical pairs within the so-called solvent cage. In this study, we prepared and investigated molecular dyads capable of producing reduced metal complexes via an indirect pathway relying on a sequence of energy and electron transfer processes between a Ru complex and a covalently connected anthracene moiety. Our test reaction to establish the proof-of-concept is the photochemical reduction of ruthenium(tris)bipyridine by the ascorbate dianion as sacrificial donor in aqueous solution. The photochemical key step in the Ru-anthracene dyads is the reduction of a purely organic (anthracene) triplet excited state by the ascorbate dianion, yielding a spin-correlated radical pair whose (unproductive) recombination is strongly spin-forbidden. By carrying out detailed laser flash photolysis investigations, we provide clear evidence for the indirect reduced metal complex generation mechanism and show that this pathway can outperform the conventional direct metal complex photoreduction. The further optimization of our approach involving relatively simple molecular dyads might result in novel photocatalysts that convert substrates with unprecedented quantum yields.

Introduction

Visible-light photoredox catalysis as a versatile tool in synthetic organic chemistry has attracted increasing attention in recent years,[1–8] and research on solar fuels continues to explore the possibility of harvesting sunlight to drive chemical reactions.[9–13] About half of the chemical syntheses in these fields are reductive transformations, with the most prominent key intermediates for substrate activation being one-electron-reduced Ru and Ir metal complexes. However, the direct generation of these intermediates via photoreduction of excited triplet states is usually inefficient, which is due to the heavy atom effect. Hence, a substantial part of the photons absorbed by the catalyst cannot be used productively, adversely affecting the sustainability aspect connected with photocatalysis.

The reduction of any triplet state by a sacrificial electron donor D initially gives a so-called spin-correlated radical pair (upper right corners in Schemes 1 a and b), which is, as a result of spin conversion, born in the multiplicity of its photoexcited precursor (i.e., in a triplet state).[14–16] Immediate recombination of this triplet radical pair in the solvent cage is spin-forbidden. In direct consequence, cage escape on a subnanosecond timescale producing non-correlated "free" radicals with typical lifetimes in the microsecond to millisecond range can proceed with unit inherent efficiency (η). This case of highly efficient formation of free radicals (Scheme 1 a) that can react productively with substrates has been observed for many organic molecules lacking heavy atoms.[17–19] The second case, in which a triplet of a heavy-atom containing molecule (e.g., a photoactive Ru complex M) is reduced, is more complicated. As a result of spin-orbit coupling, heavy atoms drastically accelerate radical pair intersystem crossing (ISC), such that triplet ($^3\overline{M^{\bullet-}D^{\bullet+}}$) and singlet radical pairs ($^1\overline{M^{\bullet-}D^{\bullet+}}$) interconvert right after electron-transfer quenching.[14–16] Only the latter radical pair can undergo ultrafast back electron transfer (bet) also known as in-cage or geminate recombination.[14] This unproductive pathway (highlighted with red labels in Scheme 1 b) rapidly converts the absorbed photons into heat rather than generating reactive open-shell species.

Most photoredox studies merely analyze Stern–Volmer emission quenching to provide evidence for photoinduced electron

[a] Dr. S. Neumann, Prof. Dr. O. S. Wenger, Jun.-Prof. Dr. C. Kerzig
Department of Chemistry, University of Basel
St. Johanns-Ring 19, 4056 Basel (Switzerland)
E-mail: oliver.wenger@unibas.ch

[b] Jun.-Prof. Dr. C. Kerzig
Department of Chemistry, Johannes Gutenberg University Mainz
Duesbergweg 10—14, 55128 Mainz (Germany)
E-mail: ckerzig@uni-mainz.de

Supporting information and the ORCID identification number(s) for the author(s) of this article can be found under: https://doi.org/10.1002/chem.202004638.

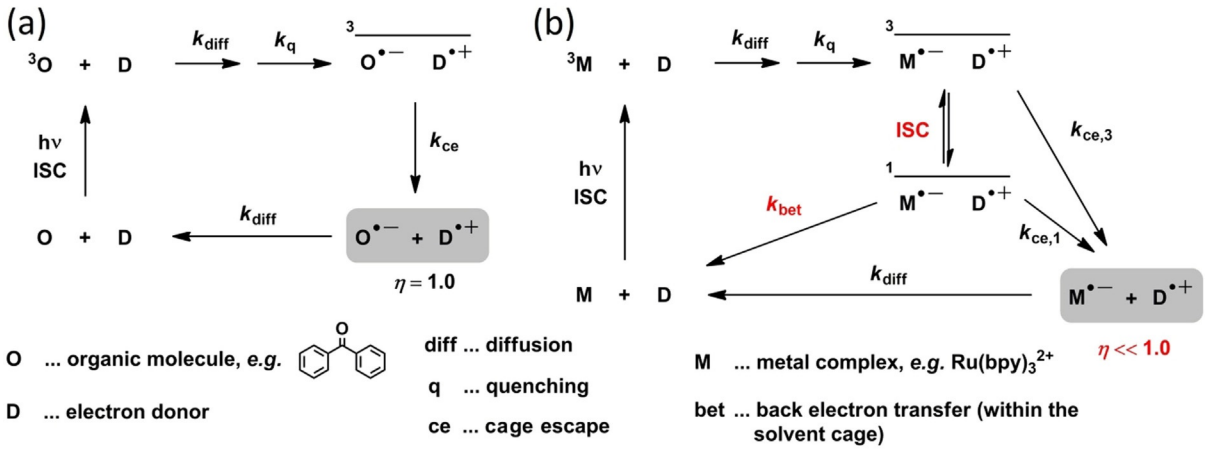

Scheme 1. Simplified representation of the triplet photoreduction of a typical purely organic chromophore (a) and a metal complex containing a heavy atom (b). The lower right corners of both sub-schemes show "free" radicals (produced through escape from the solvent cage), which can undergo subsequent reactions with additives or diffusion-mediated recombination processes. Cage escape of the spin-correlated triplet radical pair is the only pathway in (a), whereas in (b) cage escape competes with intersystem crossing of the initial radical pair followed by in-cage back electron transfer. The latter mechanism significantly reduces the inherent efficiency of the photoreduction (η).

transfer processes. However, in photochemistry one excited state quenched via photoinduced electron transfer (PET) does not necessarily mean that one reduced or oxidized species is formed. Despite practically quantitative excited-state quenching, the actual yield of free radicals or radical ions might be close to zero,[20,21] but the determination of cage-escape efficiencies η for a given PET event requires more sophisticated experimental techniques such as quantitative transient absorption spectroscopy. Owing to the lack of systematic quantitative studies in photochemistry, the exact factors that govern the overall efficiencies of PET processes are still poorly understood and a reliable prediction of the η values cannot be made in advance. For instance, the inherent photoreduction efficiencies for an anionic ruthenium(II) complex by a series of dianionic electron donors differ by as much as a factor of 30.[20] Most η values for PET reactions with triplet-excited Ru complexes are in the range from 0.05 (5%) to 0.6 (60%),[21–27] clearly indicating that unproductive in-cage recombination is a general energy-wasting problem.

In this work, we have prepared novel molecular dyads consisting of a ruthenium-(tris)bipyridine unit (M) covalently attached to an anthracene (A) moiety, and investigated their photochemical properties. Using quantitative laser flash photolysis (LFP) with optical detection of the intermediates, we will present an alternative mechanism for the generation of one-electron reduced metal complexes M$^{\bullet-}$ that is able to outperform the conventional direct photoreduction of metal complexes. The underlying key principle is that the triplet of the heavy-atom free anthracene chromophore is photoreduced and the desired species M$^{\bullet-}$ is subsequently generated by a thermal (intramolecular) electron transfer, which does not suffer from spin-dependent loss channels.

Results and Discussion

Quantitative studies on cage escape yields or inherent efficiencies for PET reactions require the determination of molar absorption coefficients of the quenching products. Reductive quenching of triplet-excited ruthenium(tris)bipyridine ^{3}Ru(bpy)$_3^{2+}$ (^{3}M) in water to yield M$^{\bullet-}$ is probably the best-investigated photoreduction of a heavy-atom containing chromophore.[22,27–31] Among the readily available sacrificial donors,[32] the ascorbate dianion Asc^{2-} is the most promising candidate for the alternative photoreduction mechanism presented herein, because of the very low potential for its oxidation. The direct photoreduction of ^{3}Ru(bpy)$_3^{2+}$ by Asc^{2-} (Scheme 2a) proceeds with an η of about 0.4;[29,30] this means that some 60% of all quenching events do not produce the desired reduced complex Ru(bpy)$_3^+$ (M$^{\bullet-}$), which is a versatile intermediate for the initiation of numerous photoredox reactions. An η increase is highly desirable since it should not only result in a significantly shorter irradiation time for a given photoreaction, but it might also increase the catalyst stability by reducing the number of unproductive photocatalyst excitation events that lead to photodecomposition.

Guided by numerous studies on metal complex-aromatic hydrocarbon dyads[33–39] as well as the photoreduction investigations of naphthalene[40] and pyrene[41] triplets, the following strategy (Scheme 2b) provides an *indirect* access to M$^{\bullet-}$ and aims to increase η by avoiding the *direct* photoreduction of ^{3}Ru(bpy)$_3^{2+}$: (1) Selective excitation of M to yield ^{3}M after ultrafast ISC, (2) intramolecular triplet-triplet energy transfer (TTET) producing ^{3}A, (3) aryl radical anion generation via photoreduction of ^{3}A by Asc^{2-} (ET), (4) intramolecular electron transfer (iET) from A$^{\bullet-}$ to M yielding M$^{\bullet-}$. In principle a strongly related reaction sequence could occur with both unconnected chromophores,[41–44] but the linkage of the metal complex and the aromatic hydrocarbon unit in a dyad greatly enhances the overall efficiency as slow diffusion between desired reaction

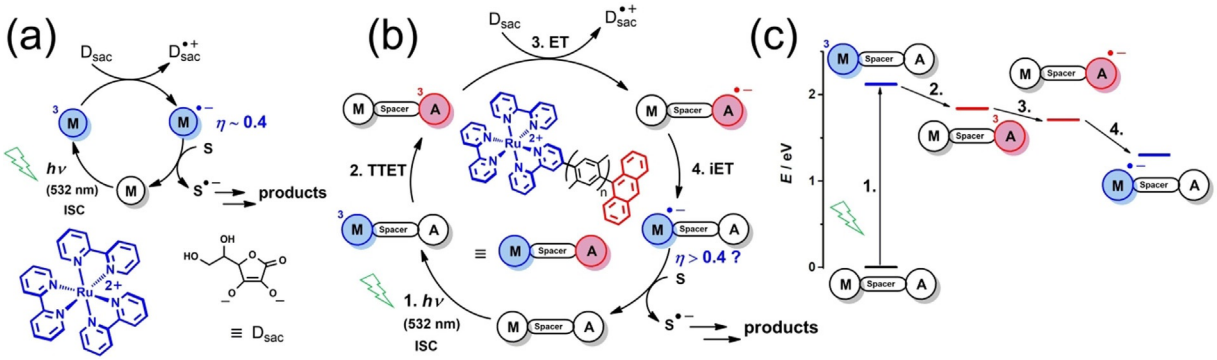

Scheme 2. (a) Mechanism of the conventional, but inefficient photochemical generation of one-electron reduced $Ru(bpy)_3^{2+}$ ($M^{\bullet-}$) by reductive triplet quenching with the ascorbate dianion as sacrificial donor and catalytic substrate (S) activation by $M^{\bullet-}$. (b) Novel indirect mechanism for the visible-light driven $M^{\bullet-}$ generation in $Ru(bpy)_3^{2+}$-anthracene (M-A) dyads with different numbers n of *p*-xylene spacers ($n = 1, 2$). (c) Energy diagram for the four key steps of the mechanism shown in (b). Pertinent triplet energies and redox potentials were taken from the literature.[31,45,46]

partners, which would compete with photophysical deactivation or radical recombination, is superfluous in our molecular dyads. All key steps are thermodynamically feasible (Scheme 2c) and the specific design of our molecular dyads is discussed in the next section. Interestingly, our approach is based on a "ping-pong" effect of energy and electron transfer in a molecular donor–acceptor system, which might be important for other applications beyond those related to photocatalysis: The donor of energy transfer is the acceptor of electron transfer.

Molecular design and ground state properties of the dyads

Aiming to produce a reduced ruthenium complex in a dyad, the first component of the dyad is predefined. We selected anthracene as second component serving as energy acceptor and redox relay on the following grounds: (i) Previous studies on molecular dyads reported very efficient anthracene triplet formation via TTET upon visible-light excitation of ruthenium(tris)diimine complexes.[47–51] (ii) The lowest triplet in these dyads is purely anthracene-localized and lives for at least several tens of microseconds at room temperature,[47,49,50] ensuring sufficient time for reductive quenching (reaction step 3 in Scheme 2b). (iii) Inherent PET efficiencies (η) close to unity have already been observed for one-electron oxidations of anthracene-localized triplets.[48,49,52,53] Consequently, steps 1–3 in Scheme 2b/c are expected to proceed with very high efficiencies.

Most prior investigations on $Ru(bpy)_3^{2+}$-anthracene dyads employed flexible spacers between the two chromophores.[48,50,51,53] However, dyads with flexible bridging units may exist in several different conformations including conformers with very short heavy atom (Ru)-anthracene distances. To avoid this potentially detrimental situation, which might promote rapid radical pair ISC,[49] we employed *p*-xylene spacers (see Scheme 2b) to ensure rigid structures with well-defined interchromophore distances. According to our DFT calculations (see Section S3 of the Supporting Information) the Ru-anthracene distance is 12.6 Å in our dyad with one bridging unit ($Ru(bpy)_3^{2+}$-xy_1-Ant), whereas that distance amounts to 16.9 Å in the dyad with two *p*-xylene spacers ($Ru(bpy)_3^{2+}$-xy_2-Ant). The dyads have been converted into their readily water-soluble nitrates by adding aq. KNO_3 to the eluent mixture during the chromatographic purification of the final complexes. Synthetic procedures and characterization data can be found in Section S2 of the Supporting Information.

The UV/Vis absorption spectra of both dyads in aqueous solution are displayed in the upper panel of Figure 1. A comparison of these spectra with those of the reference compounds—$Ru(bpy)_3^{2+}$ (blue line in Figure 1) and anthracene-9-propionate (purple line in Figure 1), which is a water-soluble anthracene derivative—clearly indicates the presence of both chromophores in the two dyads. The dyad spectra are basically a superposition of the individual $Ru(bpy)_3^{2+}$ and anthracene spectra. This is due to the nature of the *p*-xylene spacers, as they do not significantly affect the electronic properties of covalently attached chromophores.[54–57] In line with the expected poor orbital overlap, our DFT calculations (Supporting Information, Section S3) predict average equilibrium torsion angles between the *p*-xylene planes and the adjacent π-systems of the two chromophores on the order of 70°. Moreover, the computed

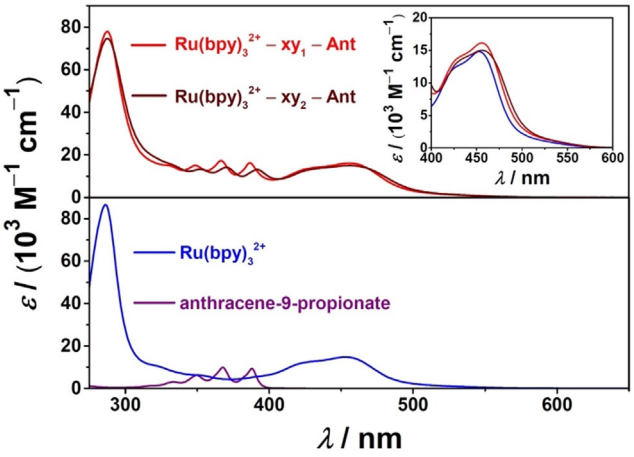

Figure 1. Calibrated UV/Vis absorption spectra of the two dyads (upper panel) and reference compounds (lower panel) in water containing 50 mM NaOH. The inset in the upper panel shows the MLCT absorption bands of the complexes on enlarged scale with the same color code as in the main plots. The *p*-xylene spacers do not absorb in the displayed spectral range.

frontier orbitals (Supporting Information, Figure S2) are either purely $Ru(bpy)_3^{2+}$ (LUMO) or anthracene (HOMO) localized, without any noticeable orbital coefficients on the *p*-xylene bridging units. A closer look at the MLCT absorption bands (inset of Figure 1) reveals a minor red-shift (about 5 nm) for the dyads compared to conventional $Ru(bpy)_3^{2+}$ as well as very similar molar absorption coefficients. We, therefore, assume that the excited-state energies and redox potentials of the individual chromophores do not significantly alter in our dyads, and we took the pertinent literature values for $Ru(bpy)_3^{2+}$ and anthracene (see energy diagram in Scheme 2c). All steady-state (Figure 1) and time-resolved (Figure 2 and Figure 3) absorption investigations of this study were carried out in alkaline MilliQ water (50 mM NaOH, pH ~ 12.7). Working under these conditions ensures the presence of our electron donor ascorbate in its highly reactive dianionic form Asc^{2-} (pK_2 = 11.4,[46] more than 95% of Asc^{2-} in the acid-base equilibrium at pH 12.7), and does not negatively influence our photoredox systems shown in Scheme 2 in any way.

Intramolecular triplet energy transfer

Selective excitation of the red edge of the MLCT absorption band[58] of both dyads with green (532 nm) laser pulses is feasible, as the UV/Vis spectra in Figure 1 clearly show. We expect the ^{1}MLCT-excited Ru complex in the dyads to undergo ultrafast[59] and quantitative[60] ISC to give a ^{3}MLCT state, similar to what has been observed for free $Ru(bpy)_3^{2+}$, because compet-

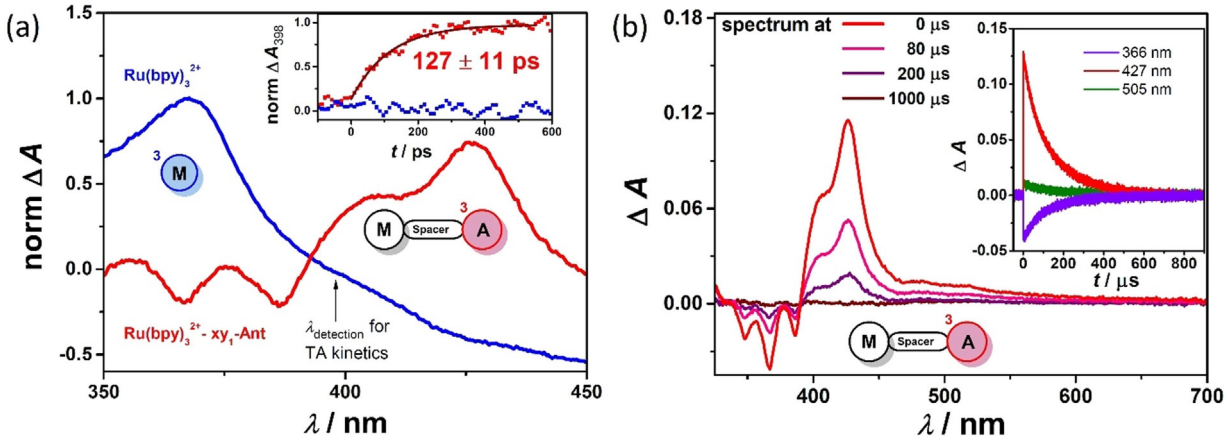

Figure 2. Transient absorption investigations on $Ru(bpy)_3^{2+}$-xy_1-Ant showing fast anthracene triplet formation via intramolecular TTET (a) and its decay on a ns-to-ms timescale (b), both upon visible light excitation of the dyad in Ar-saturated water containing 50 mM NaOH. (a) Main plot, transient absorption spectra of the dyad and $Ru(bpy)_3^{2+}$ as reference. Excitation was carried out with 455 nm laser pulses (~30 ps, 1 mJ); detection occurred by time-integration between 3 and 5 ns after the laser pulse. Inset, time-resolved transient absorption traces recorded at 398 nm (isosbestic point between $Ru(bpy)_3^{2+}$ and $^3Ru(bpy)_3^{2+}$) showing the triplet anthracene formation kinetics. (b) Main plot, transient absorption spectra time-integrated over 200 ns with different delay times relative to the 532 nm laser flash (~10 ns, 28 mJ); a 30 µM $Ru(bpy)_3^{2+}$-xy_1-Ant solution was used. Inset, kinetic transient absorption traces at different detection wavelengths. For further explanations, see the main text.

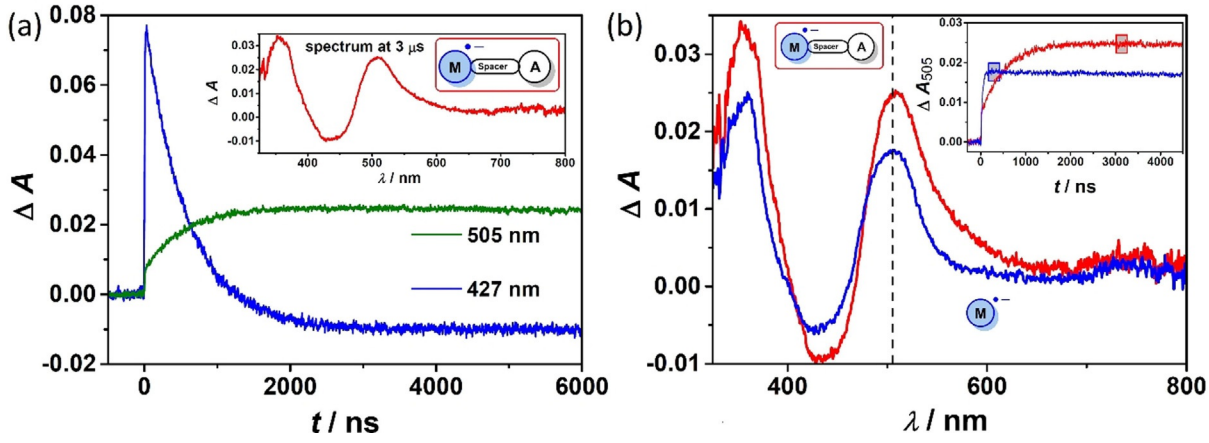

Figure 3. Reduction of $Ru(bpy)_3^{2+}$-xy_1-^{3}Ant by the ascorbate dianion Asc^{2-} (a) and comparative experiments on the formation of one-electron reduced metal complexes $M^{\bullet-}$ using $Ru(bpy)_3^{2+}$-xy_1-Ant and $Ru(bpy)_3^{2+}$ (b) upon 532 nm excitation (~10 ns, 20 mJ) of Ar-saturated aqueous solutions containing 50 mM NaOH. The complex concentrations were adjusted such that both dyad and reference solutions have identical absorptions at the excitation wavelength (A_{532} = 0.026). (a) Main plot, kinetic transient absorption traces at the absorption maximum of the anthracene triplet (blue) and the long-wavelength absorption band of $M^{\bullet-}$ (green). Inset, transient absorption spectrum of the quenching product(s) time-integrated over 200 ns. (b) Main plot, transient absorption spectra of $M^{\bullet-}$ (dyad, red, 4.7 mM Asc^{2-}; $Ru(bpy)_3^{2+}$, blue, 9.6 mM Asc^{2-}) recorded with the detection windows highlighted in the inset. The dashed vertical line in the main plot indicates the detection wavelength for the kinetic traces of the inset.

ing energy (FRET) or electron transfer mechanisms with the covalently connected anthracene moiety can be ruled out for thermodynamic reasons.[45] Indeed, very weak ^{3}MLCT emission was observed during steady-state luminescence spectroscopy with deoxygenated $Ru(bpy)_3^{2+}$-xy_1-Ant solutions, but a comparison with the parent compound $Ru(bpy)_3^{2+}$ under identical excitation and detection conditions demonstrates that the dyad is less emissive by about two orders of magnitude. Initial time-resolved emission experiments on $Ru(bpy)_3^{2+}$-xy_1-Ant upon excitation with 532 nm laser pulses of ~10 ns duration showed an instrumentally limited decay of the ^{3}MLCT emission (detection wavelength, 600 nm). These results provide unambiguous evidence for fast and efficient ^{3}MLCT quenching in our dyad, given that the unquenched ^{3}MLCT lifetime of free $Ru(bpy)_3^{2+}$ is about 600 ns under these experimental conditions.[37,61] To characterize the quenching process and the resulting product, we carried out transient absorption investigations on short (Figure 2a) and long (Figure 2b) timescales. The experimental section with pertinent descriptions of the employed instruments as well as the underlying methods is given in the Supporting Information (Section S1.2).

Figure 2a displays picosecond transient absorption studies of deoxygenated $Ru(bpy)_3^{2+}$-xy_1-Ant and $Ru(bpy)_3^{2+}$ solutions at room temperature, which were excited with ~30 ps pulses at 455 nm. We first investigated $Ru(bpy)_3^{2+}$ and reproduced the well-known transient absorption spectrum of its ^{3}MLCT state ($^3Ru(bpy)_3^{2+}$) with a pronounced absorption band at ~370 nm and the characteristic ground state bleach in the blue region of the visible spectrum (blue spectrum in Figure 2a); both absorption features are produced instantaneously with our time resolution and remain persistent in the employed 5 ns time window.[62] We speculated that the isosbestic point of $Ru(bpy)_3^{2+}$ and $^3Ru(bpy)_3^{2+}$ at 398 nm (compare, blue spectrum and kinetic trace in Figure 2a), which should also exist in the dyad, may be useful for studying the intramolecular quenching reaction (TTET from $^3Ru(bpy)_3^{2+}$ to anthracene, step 2 in Scheme 2b, c) in isolation. Kinetic absorption measurements with the dyad $Ru(bpy)_3^{2+}$-xy_1-Ant show a clear first-order signal rise at this main detection wavelength (detection window, 390–405 nm) with a time constant of about 130 ps (inset of Figure 2a). Practically identical time constants were observed at the ^{3}MLCT absorption maximum (360–375 nm) and in the spectral range of the $Ru(bpy)_3^{2+}$ ground state bleach (450–475 nm).

The transient absorption spectrum of $Ru(bpy)_3^{2+}$-xy_1-Ant obtained with a time delay ensuring quantitative $^3Ru(bpy)_3^{2+}$ quenching shows a clear (fine-structured) bleach in the near UV along with an intense absorption band with a maximum at 427 nm and a shoulder at 406 nm (Figure 2a, red spectrum), resembling the reported triplet-triplet absorption spectra of several anthracene derivatives.[45,63–66] These findings are in perfect agreement with a purely anthracene-localized triplet state as TTET quenching product. The reverse TTET from the anthracene triplet (triplet energy, ~1.84 eV)[45] to the ruthenium complex (triplet energy, ~2.12 eV)[58] is endergonic by almost 0.3 eV, hence this reaction does not play any noticeable role in our dyad. Sub-100 ps (forward) energy transfer kinetics were reported for related ruthenium complex-arene dyads.[51,67] In these dyads, the two chromophores were either directly connected[67] or a short flexible spacer[51] was used. A longer interchromophore distance and less pronounced orbital overlap can be expected for $Ru(bpy)_3^{2+}$-xy_1-Ant, which might explain the slightly lower energy transfer rate that we observed in Figure 2a (127 ps). However, TTET in $Ru(bpy)_3^{2+}$-xy_1-Ant is faster by about two orders of magnitude compared to rhenium(I) complex-anthracene dyads, probably due to inverted driving force effects for the latter.[68]

After switching to our nanosecond laser setup (~10 ns laser pulse duration), we observed the very same transient absorption features of the sensitized anthracene triplet (Figure 2b). The formation of this species cannot be resolved with that instrument, but it allows us to monitor the decay of the anthracene-localized triplet. All absorption bands decay with very similar kinetics and return completely to the baseline on a 1 ms timescale, as is evident from the main plot of Figure 2b. Kinetic absorption traces (inset of Figure 2b) do not obey clear first-order kinetics. There is a slight admixture of second-order decay kinetics and we attribute that effect to the well-known annihilation of long-lived anthracene triplets. Time-gated emission spectra did not show delayed emission signals resulting from the annihilation product, i.e., singlet-excited anthracene, which is most likely due to intramolecular singlet energy transfer in the dyad (FRET from singlet-excited anthracene to $Ru(bpy)_3^{2+}$).[69] The natural (unquenched) triplet anthracene lifetime is on the order of 150 μs leaving ample time for bimolecular reactions with suitable electron donors.

The ^{3}MLCT lifetime decrease from ~600 ns ($Ru(bpy)_3^{2+}$) to ~130 ps (dyad) indicates quantitative ^{3}MLCT quenching (99.98%) in our dyad and based on our results, intramolecular TTET is the only quenching pathway. Therefore, it seems natural to assume a triplet anthracene formation quantum yield of 100% upon visible excitation of $Ru(bpy)_3^{2+}$-xy_1-Ant, and we performed relative actinometry[70] with $Ru(bpy)_3^{2+}$ in water as widely used reference system,[29,71,72] following the methodology that we recently explained in detail.[57] Using 532 nm laser pulses for excitation, a double determination of the molar absorption coefficient of $Ru(bpy)_3^{2+}$-xy_1-^{3}Ant gave a value of 23000(±500) $M^{-1}cm^{-1}$ at the triplet anthracene absorption maximum, 427 nm. This molar absorption coefficient is comparable to those determined for other triplets of substituted anthracene derivatives,[45,73] which substantiates our interpretation of a quantitative TTET without additional loss channels.

Similar nanosecond LFP investigations with the longer dyad $Ru(bpy)_3^{2+}$-xy_2-Ant provide clear evidence for the fast sensitized triplet anthracene formation (TTET in Scheme 2b), but they gave unexpectedly weak triplet anthracene signals for this dyad. Under identical excitation conditions (dyad absorption at the excitation wavelength and laser pulse energy, see Supporting Information, Figure S4 for details), the triplet anthracene signals for $Ru(bpy)_3^{2+}$-xy_2-Ant are less intense by as much as a factor of three, compared to those of the $Ru(bpy)_3^{2+}$-xy_1-Ant dyad (Figure 2). We regard it as very unlikely that the molar absorption coefficients of both anthracene triplets differ significantly, in particular as their spectral shapes

are virtually identical (Figure S4). Aggregation induced quenching might provide an explanation. The surfactant-like structure of $Ru(bpy)_3^{2+}$-xy_2-Ant with the hydrophilic $Ru(bpy)_3^{2+}$ chromophore as potential head group and the long hydrophobic π-system could promote the formation of aggregates or micellar structures. $Ru(bpy)_3^{2+}$-xy_2-Ant is readily water-soluble at the typical concentrations of our experiments (~30 μM), but foam formation was clearly observed during Ar purging of the dyad solutions. The latter observation is in line with detergent properties of the longer dyad and might explain the seemingly low triplet anthracene formation efficiency observed for that compound. Further results that substantiate aggregation phenomena with $Ru(bpy)_3^{2+}$-xy_2-Ant are discussed in the next section.

The results of this section, however, demonstrate that (i) the visible-light driven sensitization of the anthracene triplet is feasible with the novel dyads and (ii) that the shorter dyad $Ru(bpy)_3^{2+}$-xy_1-Ant is a promising candidate for the mechanism of Scheme 2, since the visible-light driven formation of the long-lived anthracene-localized triplet is both fast and quantitative.

Reductive quenching and formation of reduced metal complexes

The ascorbate dianion Asc^{2-} with its redox potential of $E_{1/2}$ ($Asc^{\bullet-}/Asc^{2-}$) = 0.015 V vs. NHE[74] is a very potent electron donor. This reductant is evidently capable of reducing ^{3}MLCT-excited ruthenium complexes with essentially diffusion-controlled kinetics.[29,30] Furthermore, Asc^{2-} should be able to quench the anthracene triplet reductively (step 3 in Scheme 2b), since its triplet energy (1.84 eV) slightly surpasses the sum of the potentials for Asc^{2-} oxidation (0.015 V)[74] and anthracene reduction (1.71 V vs. NHE).[45] We indeed observed efficient quenching of the anthracene-localized triplet in $Ru(bpy)_3^{2+}$-xy_1-Ant, as the blue trace in Figure 3a illustrates. The anthracene triplet lifetime is reduced from about 150 μs to less than 1 μs, indicating complete quenching (>99%). A new species is formed with the same rate as the $Ru(bpy)_3^{2+}$-xy_1-^{3}**Ant** decay (green trace in Figure 3a). A Stern–Volmer analysis of the purely dynamic quenching yielded a rate constant of $3.6\times10^8\ M^{-1}s^{-1}$. The transient absorption spectrum right after the quenching process (inset of Figure 3a) does not show the absorption bands derived from the initial quenching product, i.e., the anthracene radical anion $A^{\bullet-}$ (maxima at ~700 nm and ~360 nm).[75,76] However, the spectroscopic signatures of the reduced metal complex $M^{\bullet-}$ ($Ru(bpy)_3^{+}$) are clearly observable, with characteristic bipyridine radical anion bands at 505 nm and 360 nm (superimposed by the ascorbate radical anion)[77] as well as the bleach of the MLCT absorption band of the parent ruthenium(II) complex.[30,78] These results can be rationalized by a fast intramolecular electron transfer from the anthracene radical anion to the metal complex unit of the dyad (step 4 in Scheme 2b). The arene radical anion is significantly higher in energy than $M^{\bullet-}$ (Scheme 2c), and we expect the intramolecular electron transfer between $A^{\bullet-}$ and M to occur on a (sub)nanosecond timescale.[79] The direct observation of the anthracene radical anion would thus not even be possible with much higher concentrations of the reductive quencher Asc^{2-}, because the monomolecular $A^{\bullet-}$ decay is always faster than its bimolecular formation (i.e., detectable anthracene radical anion concentrations cannot be formed for kinetic reasons). Nevertheless, the transient absorption studies of Figure 3a provide clear evidence for reductive quenching of the anthracene triplet and the formation of the desired reduced ruthenium complex $M^{\bullet-}$ as ultimate photoproduct in the dyad.

Figure 3b compares the $M^{\bullet-}$ formation results obtained for $Ru(bpy)_3^{2+}$ (blue) and our shorter dyad $Ru(bpy)_3^{2+}$-xy_1-Ant employing Asc^{2-} as reductive quencher. To obtain conditions allowing a quantitative interpretation of the results, we (i) have chosen complex/dyad concentrations such that both solutions have identical absorbances at our excitation wavelength (532 nm), (ii) used a constant laser pulse energy throughout this series of experiments and (iii) doubled the Asc^{2-} concentration for the well-characterized $Ru(bpy)_3^{2+}$ reference system. Not only do these conditions ensure identical triplet excited state concentrations right after the green laser pulses, but they also permit quantitative triplet quenching by the reductant Asc^{2-} in both cases. The transient absorption spectra of the main plot of Figure 3b were recorded after the completion of reductive triplet quenching (zones marked in gray in the inset). The spectral shapes of the absorption bands, their positions as well as their relative intensities are almost identical. Based on these observations, we make the reasonable assumption of essentially identical molar absorption coefficients for $M^{\bullet-}$ regardless of whether the reduced complex is derived from conventional $Ru(bpy)_3^{2+}$ or the dyad $Ru(bpy)_3^{2+}$-xy_1-Ant. Hence, $M^{\bullet-}$ formation is in fact more efficient when using the dyad (Figure 3b), and the comparison of the signal intensities directly yields the relative inherent photoreduction efficiencies η. Taking the relative transient absorption values at the minimum (~430 nm) and at both maxima (~505 and ~355 nm), we find that η for $Ru(bpy)_3^{2+}$-xy_1-Ant is higher than that for $Ru(bpy)_3^{2+}$ by 48(±14)%. With the averaged literature η value for the $Ru(bpy)_3^{2+}$ photoreduction by the ascorbate dianion (η = 0.43)[29,30] as reference, the photoreduction efficiency of the novel system, in which an anthracene triplet is reduced, amounts to about 0.64.

In a second comparison experiment, we employed the calibrated triplet anthracene ^{3}A absorption band of the dyad as internal reference signal ($23\,000\ M^{-1}cm^{-1}$ at 427 nm) and compared its intensity to that of the absorption band of the photoproduct $M^{\bullet-}$ in the green spectral region. For that, we took the difference molar absorption coefficient of $Ru(bpy)_3^{+}$ ($M^{\bullet-}$) at 505 nm ($\Delta\varepsilon = 14\,200\ M^{-1}cm^{-1}$)[29,30,80] and calculated the relative concentrations of the anthracene triplet [from the amplitude of the blue trace in Figure 3a (t = 0 value)] and the photoproduct $M^{\bullet-}$ in the dyad (from the constant ΔA value after quenching in the green trace in Figure 3a). This procedure gave an η of 0.52 from the ratio between the concentrations of $M^{\bullet-}$ and ^{3}A. The averaged η resulting from our two independent determination methods is thus 0.58±0.08.

This finding of an increased η in the dyad compared to free $Ru(bpy)_3^{2+}$ represents clear evidence that a sophisticated *indirect* reaction sequence with several steps can be more efficient

than a *direct* single-step process with a large driving force (compare, Scheme 2), reminiscent of the antenna system and the redox cofactor chain in bacterial photosynthesis. In principle, our indirect visible light driven mechanism for the formation of $M^{\bullet-}$ should be able to occur with up to unit inherent efficiency. A special geometrical arrangement between the ascorbyl radical and the reduced dyad might provide an explanation for the observable η of 0.58 in our case (Figure 4). Directly after the triplet anthracene reduction by Asc^{2-}, the corresponding triplet radical pair is formed, and as indicated above, an ultrafast intramolecular electron transfer generates the reduced metal complex in that spin-correlated radical pair. Owing to Coulombic interactions, both between $Ru(bpy)_3^{2+}$/Asc^{2-} before the quenching event and between $Ru(bpy)_3^{+}$/$Asc^{\bullet-}$ after quenching, a rather close proximity between the two unpaired electrons and the heavy atom is assumed (see Figure 4). Such an arrangement could accelerate radical pair ISC and subsequent unproductive recombination processes, which compete with the desired cage escape producing free radical species.

In order to test this hypothesis and to find a system with η values as high as for purely heavy-atom free systems, we carried out similar laser experiments as in Figure 3 with the longer dyad $Ru(bpy)_3^{2+}$-xy_2-Ant (see Supporting Information, Figure S5). As a result of the longer bridging unit, the ascorbyl radical produced via triplet anthracene quenching is expected to be more separated from the cationic ruthenium complex moiety thereby facilitating cage escape. In addition to the already mentioned unexpected findings that point to aggregation phenomena between $Ru(bpy)_3^{2+}$-xy_2-Ant dyad molecules, we observed static quenching of the dyad triplet by Asc^{2-} and a slight change in the UV/Vis spectrum of $Ru(bpy)_3^{2+}$-xy_2-Ant upon Asc^{2-} addition (see Supporting Information, Figure S6); both observations are in line with dyad-quencher preaggregation. The formation of $M^{\bullet-}$ in the longer dyad is still feasible with the ascorbate dianion as quencher, but the estimated η for this system is as low as ~0.25 (Supporting Information, Section S4). We conclude that the aggregation and static quenching phenomena observed for this dyad make this compound unsuitable for exploring our concept of indirect $M^{\bullet-}$ formation further, and thus the insight gained from $Ru(bpy)_3^{2+}$-xy_2-Ant is limited. However, comparative DFT calculations on the one-electron reduced species derived from the parent ruthenium complex and both dyads were carried out. The spin density distributions for all energy-minimized open-shell structures are very similar (Supporting Information, Figure S3), and therefore these calculations support our experimental observations that $M^{\bullet-}$ is the final quenching product in all cases.

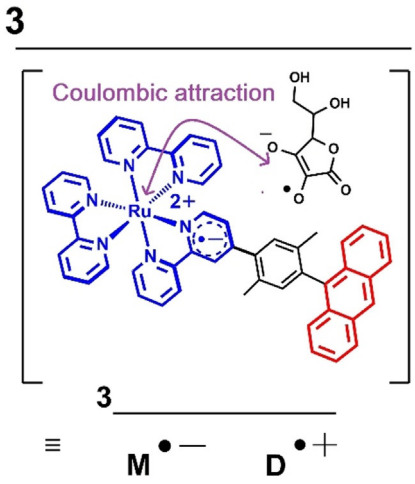

Figure 4. Possible arrangement of the ascorbyl radical anion and the one-electron reduced dyad $Ru(bpy)_3^{+}$-xy_1-Ant in the (triplet) radical pair that might result in ISC of the radical pair followed by unproductive recombination. Further explanation, see text.

The quest for other water-soluble reductive quenchers that can reduce both ^{3}MLCT and ^{3}Ant was unsuccessful, in particular as the low excited state reduction potential of the anthracene triplet (about 0.1 V vs. NHE) militates for unusually strong reductants. Related spectroscopic studies were carried out with oxidative quenching of ruthenium complex-anthracene dyads some decades ago,[48,49,53] when the power of photoredox catalysis was still hidden. Our proof-of-concept study for a more efficient indirect reductive quenching pathway avoiding the inefficient direct photoreduction of heavy-metal containing chromophores indicates that the molecular dyad approach could be developed into a general concept for improving the inherent efficiencies of PET reactions. This would have far-reaching implications for photocatalytic applications. The anthracene-containing dyads exhibit limited photostability, especially in the presence of dissolved oxygen (see Supporting Information for details). The exploitation of molecular dyads comprising a well-established 4d or 5d metal complex and a purely organic chromophore for more efficient photocatalytic transformation thus requires the design of more robust dyad-quencher systems, and our study paves the way for this promising idea.

Finally, we compare the quenching efficiencies of triplet-excited $Ru(bpy)_3^{2+}$-xy_1-Ant with that of conventional $Ru(bpy)_3^{2+}$. Using the well-known photokinetic equations[8] together with the unquenched triplet lifetimes and the bimolecular rate constants for reductive quenching with Asc^{2-}, we simulated the quenching efficiencies as a function of the Asc^{2-} concentrations (Figure 5). The long natural lifetime of the anthracene-localized triplet in $Ru(bpy)_3^{2+}$-xy_1-Ant (red lines) clearly overcompensates the slower Asc^{2-} quenching rate constant, as is evident from the much higher quenching efficiencies for the dyad compared to the conventional complex at given quencher concentrations (compare, blue and red thin lines in Figure 5). The half-quenching concentration of Asc^{2-} is as low as 18.5 μM for the dyad, whereas that quantity is 260 μM for $Ru(bpy)_3^{2+}$. After multiplication of the quenching efficiency curves with the respective inherent PET efficiencies η, the concentration-dependent cage escape yields result (thick lines in Figure 5). These curves reflect the yields of reduced metal complexes $M^{\bullet-}$ capable of activating suitable substrates (see also panels a and b in Scheme 2) or co-catalysts. The analysis of the low Asc^{2-} concentration range in Figure 5 unambiguously establishes that $M^{\bullet-}$ formation can indeed be more efficient by an order of magnitude when using our novel dyad $Ru(bpy)_3^{2+}$-xy_1-Ant.

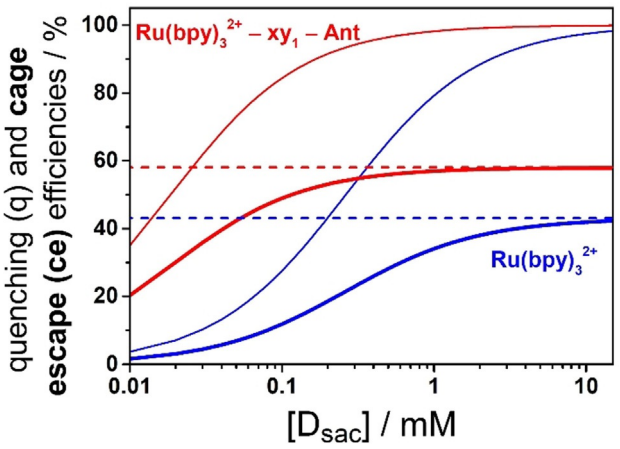

Figure 5. Comparison of quenching (thin lines) and cage escape efficiencies (thick lines) for the photoreductions of $Ru(bpy)_3^{2+}$-xy_1-Ant and $Ru(bpy)_3^{2+}$ triplets by Asc^{2-} as a function of the donor (Asc^{2-}) concentration. Parameters used for the kinetic simulations (values for the dyad shown in brackets): unquenched triplet lifetime, 0.6 μs (150 μs); quenching rate constant, 6.4×10^9 M^{-1} s^{-1}[29,30] (3.6×10^8 M^{-1} s^{-1}); inherent cage escape yield, 0.43 (0.58). See text for further details.

Conclusions

In summary, we have developed a novel mechanism for the indirect photochemical generation of one-electron reduced metal complexes $M^{\bullet-}$ (see Figure 6 for the key steps and pertinent kinetic constants), which are key intermediates in photoredox catalysis but whose direct photochemical generation is inherently inefficient.

Most studies on visible-light driven photoredox catalysis completely ignore the efficiency aspect (i.e., the overall quantum yields) and merely focus on the feasibility to use visible light as energy input. In addition to photoredox catalysis, the $M^{\bullet-}$ generation is important for many photochemical carbon dioxide reduction[12,81–83] and hydrogen production[13,84–92] mechanisms, demonstrating that the new mechanism introduced in this manuscript has several possible application areas. Our study on the heavily underexplored inherent efficiency of photoinduced electron transfer events might trigger further quantitative investigations that could contribute to a better understanding of how to use photons more efficiently,[93] which could ultimately result in more sustainability in photochemistry.[94] Elucidating the interplay of spin states, heavy atom effects and inherent reaction (rather than emission quenching) efficiencies should therefore be very important for the photochemistry of the future.[95–99] Novel molecular dyads with a visible-light-harvesting metal complex and a redox-active heavy-atom free chromophore provide a promising alternative to conventional metal complexes, as has emerged from this work.

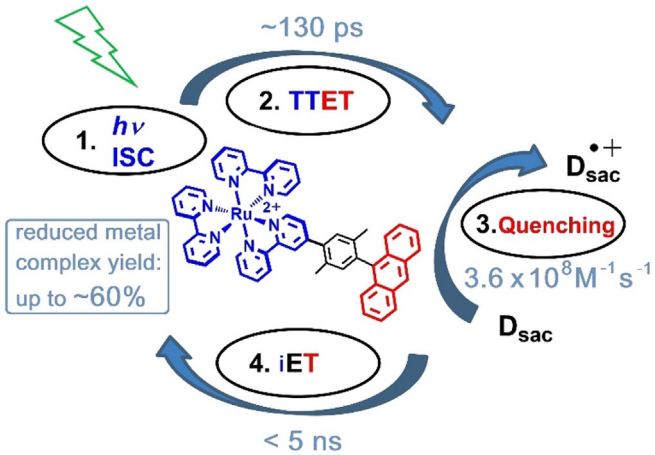

Figure 6. Simplified representation of the novel mechanism presented herein (more details are given in Scheme 2) and pertinent kinetic constants.

Acknowledgements

The authors acknowledge financial support from the Swiss National Science Foundation (grant numbers 200021_178760 and 206021_157687) and from the Swiss Nanoscience Institute (SNI Project P1406). C.K. is grateful to the German National Academy of Sciences Leopoldina (LPDS 2017-11) and the Research Fund of the University of Basel (Novartis University of Basel Excellence Scholarship for Life Sciences) for postdoc fellowships. Dr. Christopher B. Larsen is thanked for experimental support with the picosecond transient absorption measurements. Open access funding enabled and organized by Projekt DEAL.

Conflict of interest

The authors declare no conflict of interest.

Keywords: donor–acceptor systems · electron transfer · energy transfer · photocatalysis · time-resolved spectroscopy

[1] C. K. Prier, D. A. Rankic, D. W. C. MacMillan, *Chem. Rev.* **2013**, *113*, 5322–5363.
[2] M. Reckenthäler, A. G. Griesbeck, *Adv. Synth. Catal.* **2013**, *355*, 2727–2744.
[3] J. M. R. Narayanam, C. R. J. Stephenson, *Chem. Soc. Rev.* **2011**, *40*, 102–113.
[4] T. Koike, M. Akita, *Inorg. Chem. Front.* **2014**, *1*, 562–576.
[5] M. H. Shaw, J. Twilton, D. W. C. MacMillan, *J. Org. Chem.* **2016**, *81*, 6898–6926.
[6] D. M. Arias-Rotondo, J. K. McCusker, *Chem. Soc. Rev.* **2016**, *45*, 5803–5820.
[7] *Chemical Photocatalysis* (Ed.: B. König) De Gruyter, **2020**.
[8] F. Glaser, C. Kerzig, O. S. Wenger, *Angew. Chem. Int. Ed.* **2020**, *59*, 10266–10284; *Angew. Chem.* **2020**, *132*, 10350–10370.
[9] H. B. Gray, *Nat. Chem.* **2009**, *1*, 7–7.
[10] D. Gust, T. A. Moore, A. L. Moore, *Acc. Chem. Res.* **2009**, *42*, 1890–1898.
[11] F. Puntoriero, O. Ishitani, *Dalton Trans.* **2020**, *49*, 6529–6531.
[12] S. K. Lee, M. Kondo, M. Okamura, T. Enomoto, G. Nakamura, S. Masaoka, *J. Am. Chem. Soc.* **2018**, *140*, 16899–16903.
[13] T. J. Whittemore, C. Xue, J. Huang, J. C. Gallucci, C. Turro, *Nat. Chem.* **2020**, *12*, 180–185.
[14] G. J. Kavarnos, N. J. Turro, *Chem. Rev.* **1986**, *86*, 401–449.
[15] K. A. McLauchlan, U. E. Steiner, *Mol. Phys.* **1991**, *73*, 241–263.
[16] M. Goez, in *Annual Reports on NMR Spectroscopy*, Elsevier, **2009**, pp. 77–147.
[17] John. Olmsted, T. J. Meyer, *J. Phys. Chem.* **1987**, *91*, 1649–1655.
[18] E. Haselbach, E. Vauthey, P. Suppan, *Tetrahedron* **1988**, *44*, 7335–7344.
[19] M. von Raumer, P. Suppan, E. Haselbach, *Chem. Phys. Lett.* **1996**, *252*, 263–266.

[20] R. Naumann, M. Goez, *Chem. Eur. J.* **2018**, *24*, 17557 – 17567.
[21] L. Troian-Gautier, W. B. Swords, G. J. Meyer, *Acc. Chem. Res.* **2019**, *52*, 170 – 179.
[22] K. Miedlar, P. K. Das, *J. Am. Chem. Soc.* **1982**, *104*, 7462 – 7469.
[23] G. Neshvad, M. Z. Hoffman, *J. Phys. Chem.* **1989**, *93*, 2445 – 2452.
[24] M. Z. Hoffman, *J. Phys. Chem.* **1991**, *95*, 2606 – 2606.
[25] M. Georgopoulos, M. Z. Hoffman, *J. Phys. Chem.* **1991**, *95*, 7717 – 7721.
[26] A. Senz, H. E. Gsponer, *J. Phys. Org. Chem.* **1995**, *8*, 706 – 712.
[27] R. E. Adams, R. H. Schmehl, *Langmuir* **2016**, *32*, 8598 – 8607.
[28] C. R. Rivarola, S. G. Bertolotti, C. M. Previtali, *Photochem. Photobiol.* **2006**, *82*, 213.
[29] M. Goez, C. Kerzig, R. Naumann, *Angew. Chem. Int. Ed.* **2014**, *53*, 9914 – 9916; *Angew. Chem.* **2014**, *126*, 10072 – 10074.
[30] R. Naumann, C. Kerzig, M. Goez, *Chem. Sci.* **2017**, *8*, 7510 – 7520.
[31] R. Naumann, M. Goez, *Green Chem.* **2019**, *21*, 4470 – 4474.
[32] Y. Pellegrin, F. Odobel, *C. R. Chimie* **2017**, *20*, 283 – 295.
[33] X. Wang, A. Del Guerzo, R. H. Schmehl, *J. Photochem. Photobiol. C* **2004**, *5*, 55 – 77.
[34] N. D. McClenaghan, Y. Leydet, B. Maubert, M. T. Indelli, S. Campagna, *Coord. Chem. Rev.* **2005**, *249*, 1336 – 1350.
[35] F. N. Castellano, *Acc. Chem. Res.* **2015**, *48*, 828 – 839.
[36] A. J. Howarth, M. B. Majewski, M. O. Wolf, *Coord. Chem. Rev.* **2015**, *282 – 283*, 139 – 149.
[37] C. Kerzig, O. S. Wenger, *Chem. Sci.* **2018**, *9*, 6670 – 6678.
[38] Y. Sasaki, M. Oshikawa, P. Bharmoria, H. Kouno, A. Hayashi-Takagi, M. Sato, I. Ajioka, N. Yanai, N. Kimizuka, *Angew. Chem. Int. Ed.* **2019**, *58*, 17827 – 17833; *Angew. Chem.* **2019**, *131*, 17991 – 17997.
[39] X. Zhang, Y. Hou, X. Xiao, X. Chen, M. Hu, X. Geng, Z. Wang, J. Zhao, *Coord. Chem. Rev.* **2020**, *417*, 213371.
[40] C. Kerzig, M. Goez, *Phys. Chem. Chem. Phys.* **2014**, *16*, 25342 – 25349.
[41] C. Kerzig, M. Goez, *Chem. Sci.* **2016**, *7*, 3862 – 3868.
[42] I. Ghosh, R. S. Shaikh, B. König, *Angew. Chem. Int. Ed.* **2017**, *56*, 8544 – 8549; *Angew. Chem.* **2017**, *129*, 8664 – 8669.
[43] M. Marchini, G. Bergamini, P. G. Cozzi, P. Ceroni, V. Balzani, *Angew. Chem. Int. Ed.* **2017**, *56*, 12820 – 12821; *Angew. Chem.* **2017**, *129*, 12996 – 12997.
[44] M. S. Coles, G. Quach, J. E. Beves, E. G. Moore, *Angew. Chem. Int. Ed.* **2020**, *59*, 9522 – 9526; *Angew. Chem.* **2020**, *132*, 9609 – 9613.
[45] M. Montalti, A. Credi, L. Prodi, M. T. Gandolfi, *Handbook of Photochemistry*, CRC/Taylor & Francis, Boca Raton, 3rd ed., **2006**.
[46] J. J. Warren, T. A. Tronic, J. M. Mayer, *Chem. Rev.* **2010**, *110*, 6961 – 7001.
[47] J. C. Freys, O. S. Wenger, *Eur. J. Inorg. Chem.* **2010**, 5509 – 5516.
[48] S. Boyde, G. F. Strouse, W. E. Jones, T. J. Meyer, *J. Am. Chem. Soc.* **1989**, *111*, 7448 – 7454.
[49] G. J. Wilson, A. Launikonis, W. H. F. Sasse, A. W.-H. Mau, *J. Phys. Chem. A* **1998**, *102*, 5150 – 5156.
[50] G. J. Wilson, A. Launikonis, W. H. F. Sasse, A. W.-H. Mau, *J. Phys. Chem. A* **1997**, *101*, 4860 – 4866.
[51] J. R. Schoonover, D. M. Dattelbaum, A. Malko, V. I. Klimov, T. J. Meyer, D. J. Styers-Barnett, E. Z. Gannon, J. C. Granger, W. S. Aldridge, J. M. Papanikolas, *J. Phys. Chem. A* **2005**, *109*, 2472 – 2475.
[52] O. Johansen, A. W.-H. Mau, W. H. F. Sasse, *Chem. Phys. Lett.* **1983**, *94*, 107 – 112.
[53] C. Weinheimer, Y. Choi, T. Caldwell, P. Gresham, J. Olmsted, *J. Photochem. Photobiol. Chem.* **1994**, *78*, 119 – 126.
[54] S. E. Miller, A. S. Lukas, E. Marsh, P. Bushard, M. R. Wasielewski, *J. Am. Chem. Soc.* **2000**, *122*, 7802 – 7810.
[55] M. Gilbert, B. Albinsson, *Chem. Soc. Rev.* **2015**, *44*, 845 – 862.
[56] O. S. Wenger, *Acc. Chem. Res.* **2011**, *44*, 25 – 35.
[57] S. Neumann, C. Kerzig, O. S. Wenger, *Chem. Sci.* **2019**, *10*, 5624 – 5633.
[58] S. Campagna, F. Puntoriero, F. Nastasi, G. Bergamini, *Top. Curr. Chem.* **2007**, *280*, 117 – 214.
[59] N. H. Damrauer, G. Cerullo, A. Yeh, T. R. Boussie, C. V. Shank, J. K. McCusker, *Science* **1997**, *275*, 54 – 57.
[60] J. N. Demas, D. G. Taylor, *Inorg. Chem.* **1979**, *18*, 3177 – 3179.
[61] K. J. Morris, M. S. Roach, W. Xu, J. N. Demas, B. A. DeGraff, *Anal. Chem.* **2007**, *79*, 9310 – 9314.
[62] M. Skaisgirski, C. B. Larsen, C. Kerzig, O. S. Wenger, *Eur. J. Inorg. Chem.* **2019**, 4256 – 4262.
[63] R. Konuk, J. Cornelisse, S. P. McGlynn, *J. Chem. Phys.* **1986**, *84*, 6808 – 6815.
[64] Y. V. Aulin, M. van Sebille, M. Moes, F. C. Grozema, *RSC Adv.* **2015**, *5*, 107896 – 107903.
[65] V. Gray, A. Dreos, P. Erhart, B. Albinsson, K. Moth-Poulsen, M. Abrahamsson, *Phys. Chem. Chem. Phys.* **2017**, *19*, 10931 – 10939.
[66] C. Fischer, C. Kerzig, B. Zilate, O. S. Wenger, C. Sparr, *ACS Catal.* **2020**, *10*, 210 – 215.
[67] D. S. Tyson, K. B. Henbest, J. Bialecki, F. N. Castellano, *J. Phys. Chem. A* **2001**, *105*, 8154 – 8161.
[68] M. E. Walther, O. S. Wenger, *Dalton Trans.* **2008**, 6311 – 6318.
[69] T. N. Singh-Rachford, F. N. Castellano, *Coord. Chem. Rev.* **2010**, *254*, 2560 – 2573.
[70] H. J. Kuhn, S. E. Braslavsky, R. Schmidt, *Pure Appl. Chem.* **2004**, *76*, 2105 – 2146.
[71] P. Müller, K. Brettel, *Photochem. Photobiol. Sci.* **2012**, *11*, 632 – 636.
[72] M. K. Alnaed, J. F. Endicott, *J. Phys. Chem. A* **2018**, *122*, 9251 – 9266.
[73] I. Carmichael, G. L. Hug, *J. Phys. Chem. Ref. Data* **1986**, *15*, 1 – 250.
[74] P. Wardman, *J. Phys. Chem. Ref. Data* **1989**, *18*, 1637 – 1755.
[75] P. Natarajan, R. W. Fessenden, *J. Phys. Chem.* **1989**, *93*, 6095 – 6100.
[76] A. M. Funston, S. V. Lymar, B. Saunders-Price, G. Czapski, J. R. Miller, *J. Phys. Chem. B* **2007**, *111*, 6895 – 6902.
[77] M. Brautzsch, C. Kerzig, M. Goez, *Green Chem.* **2016**, *18*, 4761 – 4771.
[78] G. A. Heath, L. J. Yellowlees, P. S. Braterman, *J. Chem. Soc. Chem. Commun.* **1981**, 287 – 289.
[79] G. L. Closs, L. T. Calcaterra, N. J. Green, K. W. Penfield, J. R. Miller, *J. Phys. Chem.* **1986**, *90*, 3673 – 3683.
[80] T.-T. Tran, M.-H. Ha-Thi, T. Pino, A. Quaranta, C. Lefumeux, W. Leibl, A. Aukauloo, *J. Phys. Chem. Lett.* **2018**, *9*, 1086 – 1091.
[81] H. Hori, F. P. A. Johnson, K. Koike, O. Ishitani, T. Ibusuki, *J. Photochem. Photobiol. Chem.* **1996**, *96*, 171 – 174.
[82] X. Zhang, M. Cibian, A. Call, K. Yamauchi, K. Sakai, *ACS Catal.* **2019**, *9*, 11263 – 11273.
[83] P. Lang, R. Giereth, S. Tschierlei, M. Schwalbe, *Chem. Commun.* **2019**, *55*, 600 – 603.
[84] P. Lei, M. Hedlund, R. Lomoth, H. Rensmo, O. Johansson, L. Hammarström, *J. Am. Chem. Soc.* **2008**, *130*, 26 – 27.
[85] E. Joliat-Wick, N. Weder, D. Klose, C. Bachmann, B. Spingler, B. Probst, R. Alberto, *Inorg. Chem.* **2018**, *57*, 1651 – 1655.
[86] J. L. Dempsey, B. S. Brunschwig, J. R. Winkler, H. B. Gray, *Acc. Chem. Res.* **2009**, *42*, 1995 – 2004.
[87] J. Habermehl, D. Nauroozi, M. Martynow, Y. E. Vilk, R. Beranek, J. Guthmuller, S. Rau, *Sustainable Energy Fuels* **2020**, *4*, 619 – 624.
[88] K. Ladomenou, M. Natali, E. Iengo, G. Charalampidis, F. Scandola, A. G. Coutsolelos, *Coord. Chem. Rev.* **2015**, *304 – 305*, 38 – 54.
[89] C. Li, M. Wang, J. Pan, P. Zhang, R. Zhang, L. Sun, *J. Organomet. Chem.* **2009**, *694*, 2814 – 2819.
[90] K. Sakai, H. Ozawa, *Coord. Chem. Rev.* **2007**, *251*, 2753 – 2766.
[91] S. Pullen, H. Fei, A. Orthaber, S. M. Cohen, S. Ott, *J. Am. Chem. Soc.* **2013**, *135*, 16997 – 17003.
[92] Y. Luo, S. Maloul, S. Schönweiz, M. Wächtler, C. Streb, B. Dietzek, *Chem. Eur. J.* **2020**, *26*, 8045 – 8052.
[93] K. Ozawa, Y. Tamaki, K. Kamogawa, K. Koike, O. Ishitani, *J. Chem. Phys.* **2020**, *153*, 154302.
[94] C. G. Bochet, *Chimia* **2019**, *73*, 720 – 723.
[95] D. Guo, T. E. Knight, J. K. McCusker, *Science* **2011**, *334*, 1684 – 1687.
[96] J. H. Klein, D. Schmidt, U. E. Steiner, C. Lambert, *J. Am. Chem. Soc.* **2015**, *137*, 11011 – 11021.
[97] A. Cravcenco, M. Hertzog, C. Ye, M. N. Iqbal, U. Mueller, L. Eriksson, K. Börjesson, *Sci. Adv.* **2019**, *5*, eaaw5978.
[98] C. R. Tichnell, D. R. Daley, B. W. Stein, D. A. Shultz, M. L. Kirk, E. O. Danilov, *J. Am. Chem. Soc.* **2019**, *141*, 3986 – 3992.
[99] M. R. Wasielewski, M. D. E. Forbes, N. L. Frank, K. Kowalski, G. D. Scholes, J. Yuen-Zhou, M. A. Baldo, D. E. Freedman, R. H. Goldsmith, T. Goodson, M. L. Kirk, J. K. McCusker, J. P. Ogilvie, D. A. Shultz, S. Stoll, K. B. Whaley, *Nat. Rev. Chem.* **2020**, *4*, 490 – 504.

Manuscript received: October 20, 2020
Revised manuscript received: December 2, 2020
Accepted manuscript online: December 4, 2020
Version of record online: January 28, 2021